Robust Control Law Development for a Hypersonic Cruise Aircraft

by

Mark R. Anderson,* Abbas Emami-Naeini,#
and James H. Vincent*

Systems Control Technology, Inc.
2300 Geng Road
Palo Alto, CA 94304

Abstract

Systems Control Technology, Inc. is participating in the Air Force program entitled "Robust Control Law Development for Modern Aerospace Vehicles" (MAVRIC) as a subcontractor to Northrop Aircraft Division. The goal of this program is to apply state-of-the-art robust control law design methodologies to high-performance aircraft with significant modelling errors (uncertainties). The uncertainties which are being considered include structured, unstructured, and those due to linearization, gain scheduling, and model reduction. A model-following design technique developed under a previous Air Force study has been cast into an H^∞ synthesis framework. The design approach has the potential for direct design of control laws which feature both robust stability and performance.

Two vehicles are being considered in the MAVRIC program: a fighter aircraft with enhanced maneuverability and a hypervelocity flight vehicle. Control law development for the hypersonic vehicle will be discussed in this paper.

I. Introduction

A hypervelocity vehicle has been designed by Northrop Aircraft Division specifically for the MAVRIC program. A complete nonlinear simulation has been developed with components modeling the equations-of-motion (including a rotating earth), jet damping effects, a complete aerodynamic data base, propulsion system, sensors, actuators, and structural modes[1].

Modeling of uncertainties is a very important part of the MAVRIC program. The sources of uncertainty considered significant in the hypervelocity vehicle model development are: errors in aerodynamic prediction, variations in structural frequency, damping and mode shapes, and neglected sensor, actuator, and structural modes. The uncertainty data base is used directly in the design approach and also for stability and performance robustness evaluation[2].

It is difficult to define appropriate flight control design specifications for flight vehicles capable of hypersonic flight speeds primarily because the design experience in this flight regime is limited. The most recently developed operational aircraft capable of hypersonic flight is the Space Shuttle Orbiter. Another relevant and useful resource is the flying qualities specifications proposed for NASA's Supersonic Cruise Research (SCR) vehicle.[3] The SCR flying qualities specification was derived from the handling characteristics of some large supersonic aircraft such as the XB-70 and the Concorde. The design specifications used for the MAVRIC hypervelocity vehicle are composed of a combination of requirements chosen from the SCR specifications, the military standard aircraft specifications,[4] and published Space Shuttle design requirements.[5]

This paper will emphasize the peculiarities of controlling a hypersonic vehicle using modern H^∞ control synthesis methods. For example, it has been shown that the altitude degree-of-freedom can be very difficult to control precisely in aircraft traveling at very high speeds. The dynamics of the MAVRIC hypervelocity vehicle are also unstable in both the longitudinal and lateral-directional axes. In addition, the RCS thrusters, used to control the vehicle when conventional aerodynamic surfaces are not effective, are highly nonlinear as well as uncertain. It is expected that these inherent difficulties in controlling hypersonic aircraft will pose the biggest challenge to the modern control design methodology.

II. Technical Approach Overview

The control system for the MAVRIC hypervelocity vehicle will rely on the control structure developed for the "Design Methods for Integrated Control" (DMICS) program[6]. The DMICS control structure is shown in Figure 1. Several novel features are incorporated within this explicit model-following control structure.

---

* member, AIAA.
# member, IEEE.

The first and foremost feature is the concept of generalized controls (δ^*), that is, pure control accelerations, both translational and rotational, which can be generated by the physical control effectors. Implementation of generalized controls allows the design for mission level requirements (i.e., controlling the aircraft's spatial trajectory) to be decoupled from the design of the function level subsystems (i.e., the physical control effectors that generate the forces and moments required at the mission level). Another interesting feature of the control structure is the use of an explicit, nonlinear model for tailoring the vehicle flying qualities which is called the maneuver command generator(MCG). The control selector translates the generalized actuator commands into commands on the physical actuators.

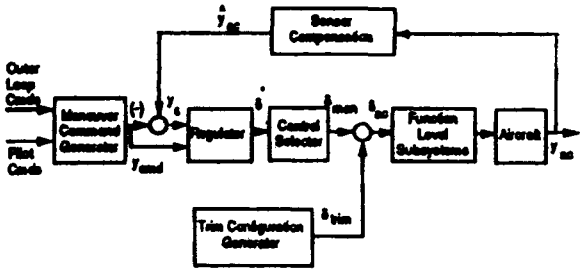

Figure 1 DMICS/MAVRIC Control Structure

The control design approach for the MAVRIC hypervelocity vehicle has evolved after several design exercises and detailed analysis of the vehicle dynamics. The current strategy is to separate the design of the feedforward controller from the design of the feedback controller. The primary purpose of the feedback controller will be to provide robust stability of the vehicle. The primary purpose of the feedforward controller is to provide robust (transient response) performance.

The feedback compensator is designed first, using the H^∞ mixed-sensitivity approach.[7] The objective of the H^∞ control methodology is to obtained a feedback compensator, call it K(s), which minimizes the H^∞ norm of the closed-loop transfer function matrix. A block diagram for the standard H^∞ control problem is shown in Figure 2. The aircraft is represented by the transfer function matrix P(s), which is composed of four blocks,

$$\begin{pmatrix} z \\ y \end{pmatrix} = P \begin{pmatrix} w \\ u \end{pmatrix} = \begin{pmatrix} P_{11} & P_{12} \\ P_{21} & P_{22} \end{pmatrix} \begin{pmatrix} w \\ u \end{pmatrix} \qquad (1)$$

The vector signal w contains all external inputs (including disturbances, sensor noise, and commands), the output z contains the response to be controlled, y is the measured variables, and u is the control input. The closed-loop transfer function matrix from the external inputs w to the controlled responses in z, denoted T_{zw}, from Figure 2 is,

$$T_{zw} = P_{11} + P_{12}(I - KP_{22})^{-1}P_{21} \qquad (2)$$

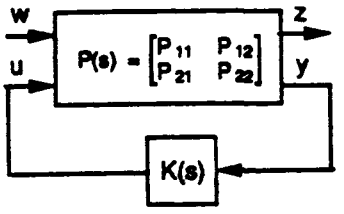

Figure 2 Standard H^∞ Control Problem

The H^∞ control methodology attempts to find the control K(s) which minimizes the the H^∞ norm of T_{zw} or,

$$\|T_{zw}\|_\infty = \min_{\omega \geq 0} \bar{\sigma}\,[T_{zw}(j\omega)] \qquad (3)$$

where, $\|T_{zw}\|_\infty$ is the notation for the H^∞ norm of the closed-loop transfer function matrix and it is defined by the largest singular value ($\bar{\sigma}$) of the transfer function matrix evaluated at positive frequencies, ω.

An interesting result of the H^∞ control theory is that when the appropriate control compensator has been found, the closed-loop transfer function matrix becomes "all-pass" which means $\bar{\sigma}\,[T_{zw}(j\omega)]$ is the same at all frequencies. As a result, the closed-loop transfer function matrix $T_{zw}(s)$ can be shaped to any form by concatenating a shaping filter, call it W(s), which models the inverse of the desired T_{zw}. The new augmented plant results in a control where $\bar{\sigma}\,[W(j\omega)T_{zw}(j\omega)]$ is all-pass. Thus, $T_{zw}(s) \approx W^{-1}(s)$ for the final control system.

The sensitivity and complementary sensitivity functions define many of the important stability and performance properties of the closed-loop system. Consequently, it becomes necessary to shape these functions to achieve optimal performance. The all-pass property of the H^∞ control methodology provides a means through which specifications on the stability and performance of the closed-loop system can be handled directly in the synthesis process.

The synthesis problem depicted in Figure 3, known as mixed sensitivity design, will be utilized to design the feedback controller for the MAVRIC hypervelocity vehicle The controlled plant for the mixed sensitivity case is,

$$P_{11} = \begin{pmatrix} W_1 \\ 0 \end{pmatrix} \qquad P_{12} = \begin{pmatrix} -W_1G \\ W_2G \end{pmatrix}$$

$$P_{21} = I \qquad P_{22} = -G \tag{4}$$

The transfer function matrix G(s) represents the airframe dynamics. The closed-loop transfer function matrix is this case is,

$$T_{zw} = \begin{pmatrix} W_1S \\ W_2T \end{pmatrix} \tag{5}$$

where $S(s) = (I + G(s)K(s))^{-1}$ is the system sensitivity function and $T(s) = I - S(s)$ is the complementary sensitivity function. The closed-loop transfer function matrix $T_{zw}(s)$ reveals weighting filters $W_1(s)$ and $W_2(s)$ which are chosen to simultaneously shape S(s) and T(s), respectively, resulting in the "mixed sensitivity" design.

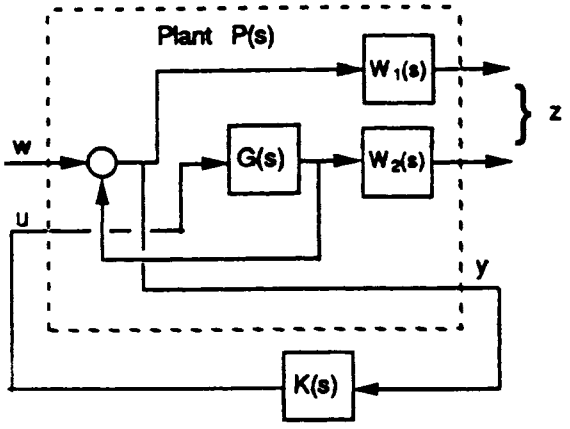

Figure 3 Mixed Sensitivity Design Diagram

The weighting filter for the complementary sensitivity function is chosen to reflect the uncertainties modeled in the feedback path. It is well known that the shape of the complementary sensitivity function dictates how large multiplicative uncertainties represented at the output of aircraft can be. Consequently, the modeled uncertainties will be reflected to the output of the aircraft to define the weighting filter $W_2(s)$.

Only bounded complex uncertainty (structured or unstructured) will be reflected to the output and used to define a complementary sensitivity function weighting. It has been found that the real parameter uncertainties in the MAVRIC hypersonic vehicle model were simply too large to be useful in defining complementary function weights. The worst-case design modeling technique will therefore be used to incorporate all real parameter uncertainty in the feedback controller design.[8]

Assuming the parameters which define the model and uncertainty are real, an approximation of the structured singular value for real uncertainty is required for evaluations. The approximation used for this paper was first published by Jones[9], although very similar approaches have been considered by Barrett[10] and Doyle[11]. The approximation for real uncertainty is,

$$\mu_R(M) = \min_{D} \max_{\Phi} \rho[-\tfrac{1}{2}\{DMD^{-1}\Phi + (DMD^{-1}\Phi)^*\}] \tag{6}$$

where,

D = real, diagonal scaling matrix
Φ = permutation matrix = diag($\pm1, \pm1, \ldots$)
ρ = spectral radius
M(s) = transfer function matrix seen by real uncertainty

The structured uncertainty approximation above reveals information needed to define the worst case design model. The magnitude of μ_R defines the uncertainty magnitude which can be tolerated by closed-loop system. The permutation matrix Φ reveals the direction of the uncertainty which might lead to instability. Consequently, the information in μ_R and Φ can be used to define the worst case design model. Specifically, the worst case design model is defined as the plant model formed by perturbing the nominal plant dynamics G(s) by the largest anticipated uncertainty magnitude in the worst direction indicated by Φ.

The feedforward controller design will be carried out by simply feeding (approximations of) commanded accelerations to the reaction control system (RCS) thrusters. The RCS thrusters will be used primarily for response quickening because the uncertainty levels of the thrusters are too large for use in the feedback loops. The feedforward controller will be designed so that the flying qualities design requirements are met with the nominal (no uncertainty) airframe dynamics. Adjustments will be made to the feedforward controller and maneuver command generator to improve transient response performance robustness, if required.

Evaluation of the resulting control laws will be carried out using singular value and structured singular value analysis.[12] In addition, the handling qualities of the aircraft will be evaluated using time and frequency responses. Eventually, the complete control systems will be implemented in a nonlinear simulation of the vehicle for nonlinear (large amplitude) signal evaluations.

III. Example Results for the Lateral-Directional-Axis

This section serves to demonstrate the control design strategy for the MAVRIC hypervelocity vehicle, lateral-directional axis. The aircraft is trimmed with a

x-body-axis acceleration of 0.35 g's and a z-body-axis acceleration of 0.33 g's. The flight condition corresponds to an ascent trajectory.

The linear, lateral-directional model includes 8 states: side velocity (ft/sec), roll rate (deg/sec), yaw rate (deg/sec), roll angle (deg), 1st asymmetric mode rate (1/sec), 1st asymmetric mode deflection, 2nd asymmetric mode rate (1/sec), and 2nd asymmetric mode deflection. The input used for control of the lateral-directional-axis is: left thrust pitch vector (deg), right thrust pitch vector (deg), left thrust yaw vector (deg), right thrust yaw vector (deg), RCS thruster up-right-center (lb), and RCS thruster up-left-center (lb). The output available for feedback control is: measured roll rate (deg/sec) and measured yaw rate (deg/sec).

The open-loop airframe eigenvalues are listed in Table 1. Note that the dutch roll mode consists of two real poles, one of which is unstable (+1.975 rad/sec). The spiral mode is also unstable, with a time-to-double of 12.5 sec. First order actuator dynamics were also included in the airframe dynamics, representing the dynamics of the thrust vectoring nozzles (0.05 sec time constant).

Table 1 Bare Airframe and Worst Case Eigenvalues

Bare-Airframe	Worst Case
0.055464	0.048221
-0.20984	-0.21022
1.9746	2.2838
-2.3255	-2.6271
-20.0	-20.0
-20.0	-20.0
-0.96210 +64.132i	-0.96210 +64.132i
-0.96210 -64.132i	-0.96210 -64.132i
-1.5270 +101.79i	-1.5270D+00 +101.79i
-1.5270 -101.79i	-1.5270D+00 -101.79i

A simple control selector was formed to blend the inputs of the airframe, to form acceleration commands. Two control selectors are used, one for feedback loops and one for feedforward signals. Only the thrust vector inputs will be utilized in the feedback paths because the RCS thrusters are highly nonlinear, with comparatively large uncertainty.

The feedback loop control selector was formed such that a generalized roll acceleration, $\dot{\delta}_{pc}$, and a generalized yaw acceleration, $\dot{\delta}_{rc}$, are commanded. The generalized roll acceleration signal will command the left and right pitch thrust vectors in opposite directions. The yaw acceleration signal will command the left and right yaw thrust vectors in unison. Scaling parameters within the control selector matrix are chosen such that a unity command acceleration yields maximum deflection of the thrust vector nozzles.

It is anticipated that a feedforward signal will be needed for roll control inputs to quicken the vehicle roll response. Therefore, the feedforward control selector will respond to a commanded roll acceleration, $\dot{\delta}_{pc}$. The feedforward commanded roll acceleration will be generated by firing the RCS thrusters aligned along the z-body-axis on the sides of the vehicle. There are 2 vernier and 2 primary thrusters located on the sides of the vehicle. The total thrust generated by each side is 1794 lb. The feedforward control selector commands 1/2 of the total thrust from each thruster when a unit roll acceleration is commanded. The total rolling moment generated by a unit roll acceleration is equivalent to one thruster generating 1794 lbs of thrust. This blending and scaling is necessary because the thrusters can only fire in one direction.

Selected uncertainties were chosen from the uncertainty model data base for synthesis and evaluation.[2] The uncertainties thought to have the greatest impact of design were considered first. The selected uncertainties are listed in Table 2, along with any weighting filter needed to describe the specific form of the uncertainty. All of the uncertainties are 1x1 blocks. Other possible uncertainties (or combinations) from the uncertainty data will be used in later evaluations.

Table 2 Selected Uncertainty Sources

Description	Scaling Filter
Weathercock stability, ΔN_β	30 %
Dihedral effect, ΔL_β	40 %
First asym. mode slope (roll)	25 %
First asym. mode slope (yaw)	30 %
Roll gyro time delay (20 msec)	$\frac{600s}{s^2+300s+30000}$
Yaw gyro time delay (20 msec)	$\frac{600s}{s^2+300s+30000}$
Roll response performance	$\frac{10}{10s+1}$
Right-side RCS thruster	0.3
Left-side RCS thruster	0.3

The first step in the synthesis procedure is to translate all of the complex uncertainties occurring in the feedback paths to the output of the vehicle. In this case, the first six uncertainties occur within the feedback loop, but only the rate gyro time delays are complex. Because the rate gyro time delays already occur at the output of the vehicle, their weights can be used directly to form the complementary sensitivity function weighting.

Figure 4 shows the frequency dependent bound of the rate gyro time delay along with a complementary sensitivity function weighting filter described by $0.01(10s+1)/(0.001s+1)*I_2$. The complementary sensitivity function weighting filter is chosen larger

than rate gyro uncertainty to insure that the mixed sensitivity controller is stable with respect to the rate gyro uncertainty.

A weighting filter for the sensitivity function is then chosen compatible to the complementary sensitivity function filter. The sensitivity function weighting filter was chosen as $\gamma(0.01s+1)/(1000s+1)*I_2$. The parameter γ was then increased until the complementary sensitivity function singular values reached their specification. The sensitivity function singular values for the initial feedback controller and nominal airframe dynamics are shown in Figure 5 for $\gamma = 2000$.

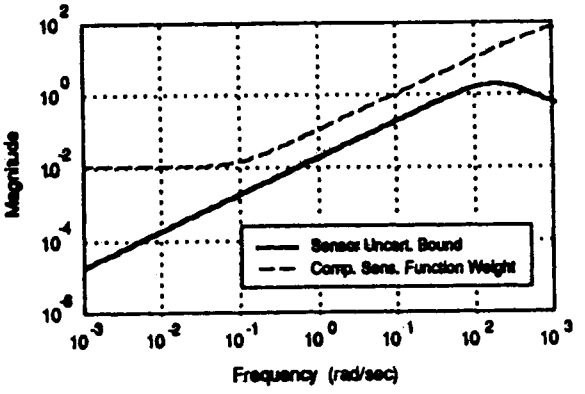

Figure 4 Sensor Uncertainty Bound

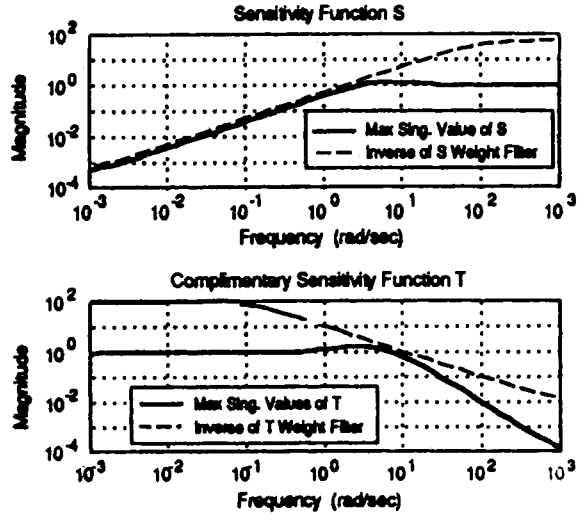

Figure 5 Initial Feedback Controller Design

The remainder of the synthesis steps require evaluation of structured singular values with several different uncertainty configurations. The graphical block diagram manipulation program Model-C® is used to form the analysis diagrams for the various uncertainty configurations. Structured singular values are computed for real uncertainty using Jones' method[9] while structured singular values for complex uncertainty are computed using Osborne's method.[13]

The initial H^∞ mixed sensitivity compensator is tested next for robustness to the real parameter uncertainties which occur in the feedback loop. The first four uncertainties listed in Table 2 are real and occur in the feedback loop. The structured singular values for these four real uncertainties are shown as the solid line in Figure 6. The peak value of about 3.2 in the structured singular value curve near 0.01 rad/sec indicates that the initial mixed sensitivity feedback controller does not have robust stability to the four real uncertainties. As a result, the worst case design model method will be used to improve the feedback compensator stability robustness properties.

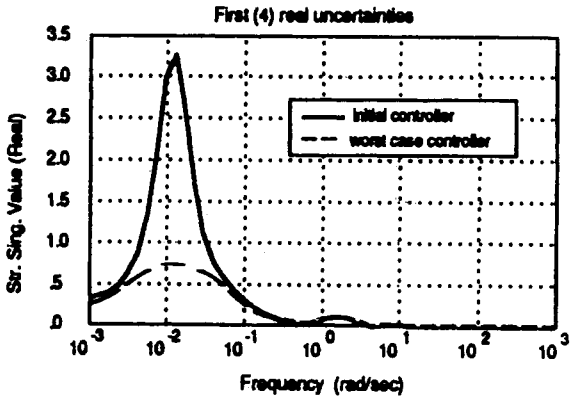

Figure 6 Stability Robustness Evaluation (Real)

The permutation matrix which defines the largest structured singular value at 0.01 rad/sec is obtained using Jones' method and is,

$$\Phi = \text{diag}\{-1, +1, +1, +1\} \qquad (3)$$

The worst case design model is defined by perturbing the airframe dynamics by a magnitude of the uncertainty indicated by the "weight" in Table 2 and in the direction (sign) indicated by the permutation matrix. Therefore, a new design model is created which includes a worst case description of the real uncertainties within the feedback loop. The eigenvalues of the worst case design model are also listed in Table 1. Note that the low-frequency (rigid-body) eigenvalues of the worst case design model are different from the low-frequency eigenvalues of the nominal bare airframe. The differences in the rigid-body eigenvalues result from the uncertainty in the weathercock stability derivative N_β and dihedral effect L_β.

Another H^∞ mixed sensitivity feedback controller is designed using the worst case design model for the sensitivity function weighting filters defined previously. Both the real and complex uncertainties present in the feedback diagram are now represented in the feedback

compensator design; the real uncertainty information is utilized in the worst case design model while the complex uncertainty is represented by the complimentary sensitivity function weighting.

Figure 6 shows the structured singular values for the first four real uncertainties with the worst case feedback controller (dashed line). One can readily see that the structured singular values with the worst case feedback controller are less than unity, indicating robust stability to the real uncertainties.

The final (worst case) feedback controller is evaluated with all of the uncertainties occurring in the feedback loop. Figure 7 shows the structured singular values for the first six uncertainties using Osborne's method. Because the peak structured singular value is less than unity, stability robustness is insured and the feedback controller design is completed.

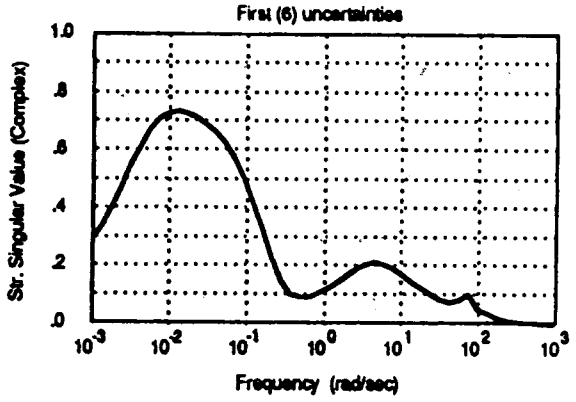

Figure 7 Final Stability Robustness Evaluation

The next step in the control design process is to design the feedforward compensator and tune the MCG to achieve nominal transient performance required by the specified flying qualities requirements. The most important response in the lateral-directional axis is the roll response to lateral stick input. Figure 8 shows the roll response of the vehicle to lateral stick inputs, both before (dotted line) and after (solid line) design of the feedforward compensator. The dashed lines in Figure 8 are the frequency domain equivalent of the roll response time response envelopes used to evaluate the Space Shuttle control system.

The feedforward compensator approximates a roll acceleration command to the feedforward control selector such that $\dot{\delta}_{pc} = (400s/(s+1000))p_c(s)$. The variable p_c is the desired roll rate produced by the MCG. The low-frequency behavior of the roll rate response was improved by including a crossfeed of $r_c(s) = (0.1/s)p_c(s)$ in the MCG.

Once nominal performance is achieved by feedforward design and MCG tuning, the control system is checked for robust transient response performance. Robust performance evaluation requires representation of the performance requirement as a fictitious uncertainty. Briefly, the model-following performance is measured by the transfer function from the commanded vehicle response to the difference between the commanded vehicle response and the actual vehicle response (the model-following error). A weighting filter is chosen to bound the largest allowable model-following error based on the frequency-domain envelopes shown in Figure 8. The performance weighting filter chosen for the hypervelocity vehicle roll rate response is $w_p(s) = 10/(10s + 1)$. Figure 9 shows the nominal airframe roll rate model-following error as the solid line while the dashed line depicts the performance weighting filter $w_p(s)$.

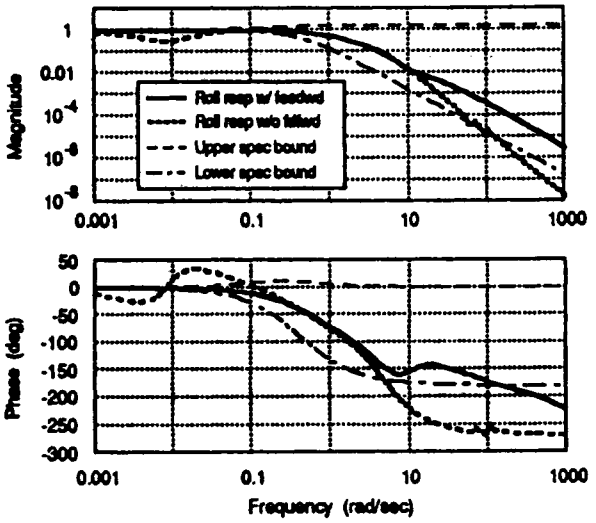

Figure 8 Feedforward Controller Design

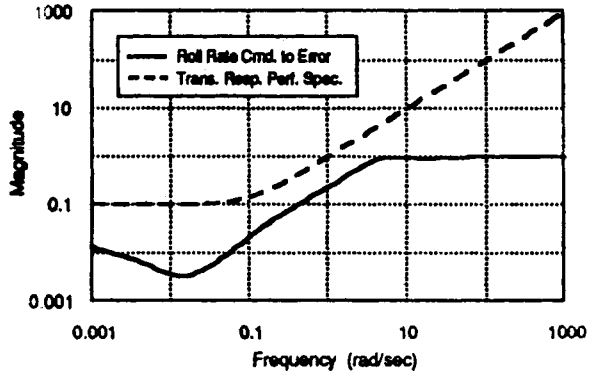

Figure 9 Roll Response Performance Weighting

The performance requirement is translated into a fictitious uncertainty by concatenating the inverse of the performance filter onto the roll rate model-following error signal. The nominal performance requirement then becomes the weighted model-following error. The nominal performance requirement is plotted in Figure

10 along with the robust performance structured singular values (complex structured singular values with all nine uncertainties listed in Table 2). One can see from the figure that the nominal performance requirement is below unity for all frequencies tested and that the robust performance structured singular values are less than unity, indicating that the closed-loop system has both robust stability and performance.

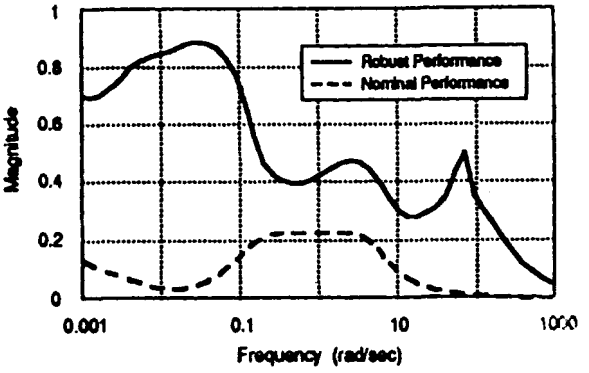

Figure 10 Final Performance Robustness Evaluation

IV. Conclusion

While the complete control system design is not yet finished, the design results achieved thusfar are very encouraging as actual uncertainties are being introduced into the design process. We feel that the most difficult part of the design approach, that is incorporating uncertainties from several sources directly in the design, has been demonstrated. In addition, the alternatives available to improve this design are clearly evident by the results completed so that success of the finished design is assured.

V. Acknowledgement

This research is currently sponsored by the U.S. Air Force, Flight Dynamics Laboratory, Wright Research and Development Center. Capt. Mary Manning and Capt. Sharon Heise have served as technical monitors. The authors would also like to thank Dr. Siva Banda and Mr. John Bowlus, also from the Flight Dynamics Laboratory, for their contributions and active support. For building the hypervelocity vehicle simulation, the efforts of the Northrop Aircraft Division, Control Systems Research personnel, including Mr. Karl Haiges (MAVRIC program manager) and Mr. Kevin Madden, are greatly appreciated.

VI. References

[1] Haiges, K.R., Tich, E.J., and Madden, K.P., "Robust Control Law Development for Modern Aerospace Vehicles Task 1: Model Development," WRDC-TR-89-3080, August 1989.

[2] Haiges, K.R., Madden, K.P., Eller, B.G., Emami-Naeini, A., Anderson, M.R., and Trankle, T.L., "Robust Control Law Development for Modern Aerospace Vehicles Task 2: Control System Criteria and Specifications," WRDC-TR-90-(draft), January 1990.

[3] Chalk, C.R., "Recommendations for SCR Flying Qualities Design Criteria," NASA CR-159236, April 1980.

[4] "Military Standard - Flying Qualities of Piloted Vehicles", MIL-STD-1797, March 1987.

[5] Myers, T.T., Johnston, D.E., and McRuer, D.T., "Space Shuttle Flying Qualities and Flight Control System Assessment Study," NASA CR-170391, June 1982.

[6] Northrop Corporation, Systems Control Technology, Inc., and General Electric Company, "Design Methods for Integrated Control Systems," AFWAL-TR-88-2061, June 1988.

[7] Safonov, M.G. and Chaing, R.Y., "CACSD Using the State-Space L^{∞} Theory - A Design Example," Proceedings of the IEEE Conference on CACSD, Washington, D.C., Sept. 1986.

[8] Anderson, M.R., "Linear Design Models for Robust Control Synthesis," AIAA Paper No. 89-3454, AIAA Guidance, Navigation, and Control Conference, Boston, MA, Aug. 1989.

[9] Jones, R.D., "Structured Singular Value Analysis for Real Parameter Variations," AIAA Paper No. 87-2589, AIAA Guidance, Navigation, and Control Conference, Monterey, CA, Aug. 1987, pp. 1424-1432.

[10] Barrett, M.F., "Conservatism with Robustness Tests for Linear Feedback Control Systems," 19th IEEE Conference on Decision and Control, Albuquerque, NM, Dec. 1980, pp. 885-890.

[11] Doyle, J.C., "Structured Uncertainty in Control System Design," 24th IEEE Conference on Decision and Control, Ft. Lauderdale, FL, Dec. 1985, pp. 260-265.

[12] Doyle, J.C., Wall, J.E., and Stein, G., "Performance and Robustness Analysis for Structured Uncertainty," Proceedings of the 21st IEEE Conference on Decision and Control, Vol. 2, Orlando, FL, Dec. 1982, pp. 629-636.

[13] Osborne, E.E., "On Pre-Conditioning of Matrices," *Journal of the Association for Computing Machinery*, Vol. 7, 1960, pp. 338-345.